Math. Model. Nat. Phenom. 15 (2020) 64
https://doi.org/10.1051/mmnp/2020047

**Mathematical Modelling of Natural Phenomena**
www.mmnp-journal.org

# CONTROL OF NIPAH VIRUS OUTBREAK IN COMMERCIAL PIG-FARM WITH BIOSECURITY AND CULLING

Samhita Das*, Pritha Das and Parthasakha Das

**Abstract.** A coupled pig-human Nipah virus disease model is studied in a commercial farm to understand dynamics of disease spillover from pig to human. To portray the specific scenario, two parameters representing biosecurity level and selective culling are included in the system. Along with standard equilibrium analysis, backward and Hopf bifurcation phenomena are demonstrated analytically and numerically. Optimal control of culling alone and also with other controls for the minimization of loss are discussed. It is observed that, irrespective of its application rate, culling is more effective in presence of other controls. Parameter sensitivity analysis of system solution has been used to identify significant parameters for the change of disease dynamics. Sensitivity test is also performed on the objective function of optimal control problem, which singled out crucial parameters influencing the economic loss of farm-owner. Based on this study, some strategies regarding application of various controls are suggested.

**Mathematics Subject Classification.** 37N25, 34D20, 49J15, 62H20.

Received May 26, 2020. Accepted November 8, 2020.

## 1. Introduction

Zoonotic pathogens have manifested as a threat to global public health since the end of last millennium. Emergence of such pathogens is attributed to climate change [14], wildlife habitat destruction and large scale farm activity [23]. Pathogens like SARS (China, 2003), Ebola (West africa, 1976), Hendra virus (Australia,1994), Marburg (central Africa, 1998) and Nipah virus (NiV) have drawn necessary attention through sporadic but fatal outbreaks. These emerging diseases have originated from wild bats [38]. Almost 60 migratory subspecies of wild bats in Africa, Indian subcontinent, south-east Asia and Australia are natural host of highly pathogenic viruses (*Paramyxoviridae, Coronaviridae, Filoviridae*). Particularly Nipah virus disease (family *Paramyxoviridae*, genus *Henipavirus*) caused a massive human fatality in its first major outbreak (Malaysia,1998). The virus itself is named from Sungai Nipah village of Malaysia where it was first identified as a new pathogen. As the human infection(257 cases, 105 deaths) spread from NiV infected pigs, massive culling of 1.1 million domestic pigs [12] was undertaken by government agency to control infection. Since then, NiV emerged abruptly from time to time in India (2001, 2007, 2018) and Bangladesh (2001–2011). In Indian sub-continent the heavily localized disease was transmitted directly to population without intermediate amplifying host (swine). The suspected

*Keywords and phrases:* Nipah virus disease, biosecurity, selective culling, backward bifurcation, Hopf bifurcation, optimal control, sensitivity analysis.

Department of Mathematics, Indian Institute of Engineering Science & Technology, Shibpur, Howrah 711103, India.

* Corresponding author: samhita_maths@yahoo.com

cause was consumption of raw date palm sap contaminated by bat excreta. The virus strain here was 91% match with the Malaysia-strain genome sequence, though the mortality rate (70%) was much higher than Malaysia (40%) [11]. It is established that wild fruit eating bats (*Pteropus sp.*) are the natural reservoirs of NiV, which can spillover to human or carrier animals (cat, dog, pig, horse). The infection leads to mild symptoms for pig with low mortality (1−5%), but causes acute respiratory and neurological complications in human [39]. There are confirmed cases of human to human infection through close contact [24]. In Malaysia slash-and-burn deforestation for plantation of palm tree and pulp wood evicted bats towards the mango orchards at the edge of pig-farms. In the most recent outbreak in Kerala (India, 2018) the loss of natural habitat of bat was the main cause, which ushered the re-emergence of the disease in India after 2007. The long distance of this location from the so called 'Nipah Belt' of south-east Asia signified the possibility of future outbreak in any region overlapped with natural territory of wild fruit bats. Some of these regions like Cambodia, Laos, Vietnam, Philippines, China have a thriving pig-farming industry [25]. Evidently, these regions are also vulnerable to epidemic similar to Malaysia. Without any vaccination or definite drug it has become extremely important to study the disease dynamics including human-livestock interaction at micro level. A mathematical model of NiV infection in commercial pig-farm will help in formulating strategy to avoid disease spillover into human settlements.

Various studies on emerging zoonotic disease dynamics using mathematical modelling has been done [7–10, 29, 40, 41]. In deterministic model the deduction of basic reproduction number [13], existence of different equilibrium points, stability analysis are covered by most studies, with some additional features like vaccination [2], relapse [1], isolation [6], optimal control [21, 22], parameter sensitivity [36] etc. Avian-human disease mechanism with two virus strains were studied by Gumel [19]. In [26], an influenza model with optimal vaccination strategy has been investigated. The NiV models are relatively less studied [4, 32]. In [32] the importance of isolation and personal hygiene is asserted in control of Nipah. Optimal control of awareness and social distancing was discussed in [3]. From all known incidents of Nipah outbreak it is evident that infected domestic pig has the biggest potential of transferring disease to human in large scale, which motivates us to study this type of two-population disease model.

Our proposed model demonstrates the NiV disease dynamics inside a medium size commercial swine-farm, where piglets are reared to a desired weight to be sold in the market. The farm workers are vulnerable to infection from pigs and prior to hospitalization, they can infect co-workers before manifestation of symptoms. The disease outbreak is ultimately responsible for an epidemic of massive scale. Inside a commercial farm the human intervention in disease dynamics can be related to farmers motivation to implement standard biosecurity measures and ethical management practices. The effective biosecurity measures include

- maintaining hygienic environment, food and water for the animals,
- regular disinfection of farm tools and vehicles,
- quarantine and observation of sick or newly procured pig,
- keeping record of sickness and death in herd,
- providing recommended vaccines and dietary supplements to the animals.

Furthermore, the owner can erect mesh nets in pig sheds to prevent bats from coming closer to the pigs, provide the workers with protective gloves and attire, as well as keep the pig herd away from fruit trees [30]. Lastly, if required, culling and proper disposal of carcasses is to be done. These measures and their degree of application is dependent on owners awareness, attitude and economic goals. So, we include a parameter named farmers control in our model which directly controls infection transmission. Mirroring the farmer's limited resource and motivation to preserve assets, culling rate is taken in the form of saturation incidence type and it is applied on only infected pig [20].

Our aim is to study the parameters significant for the existence and extinction of infection with particular importance to disease transfer from pig to farm-workers. Along with evaluation of standard basic reproduction number and existence of various equilibrium points, the backward bifurcation phenomenon has also been studied. The presence of backward bifurcation undermines the importance of basic reproduction number as the sole parameter responsible for disease eradication. Occurrence of Hopf bifurcation identifies parameter responsible

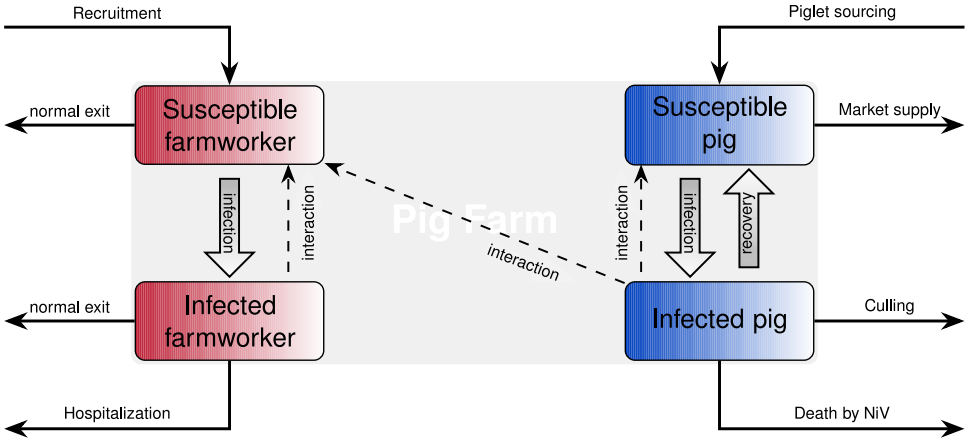


FIGURE 1. Transfer diagram of proposed model.

for persistence of disease with periodic fluctuations. A rigid deterministic model fails to take account of various realistic parametric fluctuations, which may have a decisive role in disease persistence. Using the statistical tool of Latin Hypercube Sampling (LHS) and Partial Rank Correlation Coefficient (PRCC) we perform global sensitivity analysis to single out crucial parameters for disease extinction. The long term sustainability of commercial pig farm under threat of disease will depend on its economic viability. So, there is a need of fine balance between preventive measures and destruction of livestock assets keeping owner's economic burden in mind. For this purpose we use Pontryagin's Maximum Principle [34] as a tool for optimal control of some parameters. Additionally, we look for the most important parameters responsible for economic loss using sensitivity analysis in optimal control.

The present article is organized in the following sections. The model is formulated and preliminary assumptions are stated in Section 2. Computation of basic reproduction number and existence of different equilibrium points are discussed in Section 3. Section 4 deals with backward bifurcation and Hopf bifurcation analysis. In Section 5 optimal control technique is used on the system to deduce the control rates to minimize loss. Section 6 presents numerical results and sensitivity analysis plots for the system parameters. The article ends in Section 7 with summarization of important results and conclusion.

## 2. Mathematical model formulation

The pig-human Nipah virus infection model within a commercial pig-farm is consisting of four state variables, namely, susceptible human ($S_h$), infected human ($I_h$), susceptible pig ($S_p$), infected pig ($I_p$). The following illustration (Fig. 1) depicts the interaction between different compartments of given model. The model is formulated under the following assumptions:

- The pig-farm under observation is medium sized with constant recruitment of piglets and farm-hands, where animals stay in close proximity, depicting bilinear infection rate.
- Farmers control parameter $\sigma$ can attain maximum value $\sigma_0$ ($< 1$). This control prevents spread of infection from infected pigs to workers as well as healthy pigs. It also prevents infection between workers.
- Infected workers are in contact with susceptible workers until full development of symptoms and hospitalization. They can infect humans but not pigs.
- Culling is done for only infected pigs and culling rate is considered as saturation incidence type due to limited resources to execute culling.
- As mortality rate of NiV is low for pigs, recovered pigs go back to susceptible class with chance of reinfection.

TABLE 1. Parameter definition and baseline values.

| Parameter | Description | Value range | Source |
|---|---|---|---|
| $\Lambda_h$ | recruitment rate of farm workers in pig-farm | 6−10 | Estimated |
| $\beta_1$ | NiV virus effective infection rate from human to human | 0.005−0.021 | Estimated |
| $\alpha_1$ | NiV virus effective infection rate from pig to human | 0.005−0.023 | Estimated |
| $\sigma$ | rate of farmers application of biosecurity measures (farmers control) | 0−1 | Estimated |
| $\mu_1$ | natural exit rate of workers from farm | 0.05 | Estimated |
| $\delta_1$ | hospitalization rate of workers due to NiV infection | 0.5 | [35] |
| $\Lambda_p$ | recruitment rate of pigs in farm | 20−60 | [25] |
| $\alpha_2$ | NiV effective infection rate from pig to pig | 0.043−0.075 | Estimated |
| $\mu_2$ | market supply rate of pigs | 0.042 | [16] |
| $r_2$ | recovery rate of pigs from NiV | 0.6−0.75 | Estimated |
| $\delta_2$ | death rate of pigs due to NiV | 0.01−0.05 | [39] |
| $c_2$ | culling rate of NiV infected pigs | 0−7 | Estimated |

So the formulated model is

$$\begin{aligned}
\frac{\mathrm{d}S_h\ (t)}{\mathrm{d}t} &= \Lambda_h - \beta_1\ (1-\sigma)S_h\ (t)I_h\ (t) - \alpha_1\ (1-\sigma)S_h\ (t)I_p\ (t) - \mu_1 S_h\ (t)\\
\frac{\mathrm{d}I_h\ (t)}{\mathrm{d}t} &= \beta_1\ (1-\sigma)S_h\ (t)I_h\ (t) + \alpha_1\ (1-\sigma)S_h\ (t)I_p\ (t) - \mu_1 I_h\ (t) - \delta_1 I_h\ (t)\\
\frac{\mathrm{d}S_p\ (t)}{\mathrm{d}t} &= \Lambda_p - \alpha_2\ (1-\sigma)S_p\ (t)I_p\ (t) - \mu_2 S_p\ (t) + r_2 I_p\ (t)\\
\frac{\mathrm{d}I_p\ (t)}{\mathrm{d}t} &= \alpha_2\ (1-\sigma)S_p\ (t)I_p\ (t) - r_2 I_p\ (t) - \delta_2 I_p\ (t) - c_2\frac{I_p\ (t)}{1+I_p\ (t)}
\end{aligned} \tag{2.1}$$

where the parameters are defined in Table 1.

The initial values $S_h\ (0), I_h\ (0), S_p\ (0), I_p\ (0)$ are all positive. All parameters are positive constants. Note that the animal subsystem (3rd and 4th equation of the model system) is independent of human interaction. We further denote total farm-worker population as $N_h\ (t) = S_h\ (t) + I_h\ (t)$ and total pig population in farm as $N_p\ (t) = S_p\ (t) + I_p\ (t)$ at any time $t$.

## 3. Basic reproduction number, equilibria and stability

### 3.1. Positivity and boundedness of solutions

**Lemma 3.1.** *The set* $\Theta = \left\{\ (S_h, I_h, S_p, I_p) \in \mathbb{R}^2_+ \times \mathbb{R}^2_+ : 0 < N_h \leqslant \frac{\Lambda_h}{\mu_1}\ \text{and}\ 0 < N_p \leqslant \frac{\Lambda_p}{\min\{\mu_2,\delta_2\}}\right\}$ *is compact positive invariant for the model (2.1) with positive initial conditions.*

*Proof.* It is evident if $(S_h\ (0), I_h\ (0)) \in \mathbb{R}^2_+$ and $(S_p\ (0), I_p\ (0)) \in \mathbb{R}^2_+$ the solutions of proposed model will also be positive. Adding first two equations of the system we get

$$\begin{aligned}
N_h'\ (t) &= \Lambda_h - \mu_1 N_h\ (t) - \delta_1 I_h\ (t)\\
\text{or, } N_h'\ (t) &\leqslant \Lambda_h - \mu_1 N_h\ (t)
\end{aligned}$$

Solving this inequality, we obtain $N_h\ (t) \leqslant N_h\ (0)e^{-\mu_1 t} + \frac{\Lambda_h}{\mu_1}\ (1 - e^{-\mu_1})$. Now $N_h\ (0) \leqslant \frac{\Lambda_h}{\mu_1}$ indicates that $N_h\ (t) \leqslant \frac{\Lambda_h}{\mu_1}$. Similarly from the third and fourth equation in system (2.1) we get

$$N_p'\ (t) \leqslant \Lambda_p - \mu_2 S_p\ (t) - \delta_2 I_p\ (t)$$

$$\text{or, } N_p'(t) \leqslant \Lambda_p - \min\{\mu_2, \delta_2\} N_p(t)$$

As in the human subsystem we deduce that, if $N_p(0) \leqslant \frac{\Lambda_p}{\min\{\mu_2,\delta_2\}}$, then $N_p(t) \leqslant \frac{\Lambda_p}{\min\{\mu_2,\delta_2\}}$. It is established that any solution originating in $\Theta$ will remain in the region. □

Since the proposed model is proven to be realistic in epidemic environment, we proceed to further analyze the characteristics of disease transmission.

### 3.2. Basic reproduction number and equilibrium points

The basic reproduction number of the system is calculated using next generation matrix method [37]. The disease free equilibrium is $\mathcal{D}_{00} = (\breve{S}_h, 0, \breve{S}_p, 0) = \left(\frac{\Lambda_h}{\mu_1}, 0, \frac{\Lambda_p}{\mu_2}, 0\right)$. We consider $I_h$ and $I_p$ as infected states of the system and proceed to construct standard matrices $\mathcal{F}$ and $\mathcal{V}$, which are

$$\mathcal{F} = \begin{pmatrix} \dfrac{\Lambda_h \beta_1 (1-\sigma)}{\mu_1} & \dfrac{\Lambda_h \alpha_1 (1-\sigma)}{\mu_1} \\ 0 & \dfrac{\Lambda_p \alpha_2 (1-\sigma)}{\mu_2} \end{pmatrix} \text{ and } \mathcal{V} = \begin{pmatrix} \mu_1 + \delta_1 & 0 \\ 0 & r_2 + \delta_2 + c_2 \end{pmatrix}.$$

As the Basic Reproduction Number ($R_0$) is given by the dominant eigen value of the matrix $\mathcal{F}\mathcal{V}^{-1}$, *i.e.* maximum of the two eigen values

$$R_h = \frac{\Lambda_h \beta_1 (1-\sigma)}{\mu_1 (\mu_1 + \delta_1)} \text{ and } R_p = \frac{\Lambda_p \alpha_2 (1-\sigma)}{\mu_2 (r_2 + \delta_2 + c_2)}, \tag{3.1}$$

we obtain $R_0 = \max\{R_h, R_p\}$.

Now we discuss existence of different equilibrium points. Equating the right hand side of (2.1) with 0 we obtain the following set of equations.

$$\begin{aligned} \Lambda_h - \beta_1 (1-\sigma) S_h I_h - \alpha_1 (1-\sigma) S_h I_p - \mu_1 S_h &= 0 \\ \beta_1 (1-\sigma) S_h I_h + \alpha_1 (1-\sigma) S_h I_p - \mu_1 I_h - \delta_1 I_h &= 0 \\ \Lambda_p - \alpha_2 (1-\sigma) S_p I_p - \mu_2 S_p + r_2 I_p &= 0 \\ I_p \left( \alpha_2 (1-\sigma) S_p - r_2 - \delta_2 - c_2 \frac{1}{1+I_p} \right) &= 0 \end{aligned} \tag{3.2}$$

#### *3.2.1. Boundary Equilibrium* $\mathcal{D}_{10} = (\tilde{S}_h, \tilde{I}_h, \tilde{S}_p, 0)$

Clearly for this point no disease exists among pigs ($I_p = 0$) but humans are infected ($I_h > 0$). With these conditions applied to (3.2), $\mathcal{D}_{10}$ is given by $\left(\frac{\mu_1+\delta_1}{\beta_1 (1-\sigma)}, \frac{(R_h-1)\mu_1}{\beta_1 (1-\sigma)}, \frac{\Lambda_p}{\mu_2}, 0\right)$.

**Lemma 3.2.** *$\mathcal{D}_{10}$ will exist if $R_h > 1$ and $R_p \neq 1$.*

*Proof.* From the expression of $\tilde{I}_h$, we derive the first condition. From last equation of (3.2), we see if $\alpha_2 (1-\sigma) S_p - r_2 - \delta_2 - c_2 \frac{1}{1+I_p} \neq 0$ then $I_p = 0$. This implies $\alpha_2 (1-\sigma) S_p \neq r_2 + \delta_2 + c_2$ and substituting the expression of $\tilde{S}_p$ we obtain the second condition. □

**Remark 3.3.** For the existence of other boundary equilibrium $\mathcal{D}_{01}$, it is required that $\alpha_1 = 0$. This condition uncouples the pig-human interacting system and hence not considered here.

TABLE 2. Condition of existence of endemic equilibrium in animal subsystem.

| Case | $R_p$ | $\Lambda_p$ | No. of positive $I_p$ |
|---|---|---|---|
| 1 | $> 1$ | $\leqslant \Lambda^*$ | 1 |
| 2 | $> 1$ | $> \Lambda^*$ | 1 |
| 3 | $= 1$ | $\leqslant \Lambda^*$ | 0 |
| 4 | $= 1$ | $> \Lambda^*$ | 1 |
| 5 | $< 1$ | $\leqslant \Lambda^*$ | 0 |
| 6 | $< 1$ | $> \Lambda^*$ | 0 or 2 |

*3.2.2. Endemic equilibrium* $\mathcal{D}_{11} = (\bar{S}_h, \bar{I}_h, \bar{S}_p, \bar{I}_p)$

Since $\bar{I}_p > 0$, from the last two equations of (3.2) we get,

$$\bar{S}_p = \frac{\Lambda_p + r_2\bar{I}_p}{\alpha_2\ (1-\sigma)\bar{I}_p + \mu_2} \text{and } \alpha_2\ (1-\sigma)\bar{S}_p = r_2 - \delta_2 - c_2\frac{1}{1+\bar{I}_p}. \tag{3.3}$$

From (3.3) we obtain the quadratic equation in

$$A_0\ (\bar{I}_p)^2 + A_1\bar{I}_p + A_2 = 0, \tag{3.4}$$

which will be used to find the condition of existence of endemic equilibrium. Here

$$\begin{aligned} A_0 &= \alpha_2\ (1-\sigma)\delta_2 \\ A_1 &= \alpha_2\ (1-\sigma)\ (r_2 + 2\delta_2 + c_2) + \mu_2\ (r_2 + \delta_2) - \Lambda_p\alpha_2\ (1-\sigma) \\ A_2 &= \mu_2\ (r_2 + \delta_2 + c_2)[1 - R_p]. \end{aligned} \tag{3.5}$$

From (3.5) we denote $\Lambda^* = (r_2 + 2\delta_2 + c_2) + \mu_2\ (r_2 + \delta_2)/[\alpha_2\ (1-\sigma)]$. So sign of $A_1$ is equivalent to sign of $(\Lambda^* - \Lambda_p)$. Now Descarte's rule of sign is used to determine condition of existence of at least one positive root of the quadratic equation. The results are summarized in Table 2.

For case 6, if the discriminant of (3.4), *i.e.* $A_1^2 - 4A_0A_2$ is $> 0$, only then two positive $\bar{I}_p$ will exist. This signifies existence of two endemic equilibriums in animal subsystem of the model. Simplifying the discriminant we obtain the condition as

$$\frac{\alpha_2\ (1-\sigma)\ (\Lambda^* - \Lambda_p)^2}{4\delta_2\mu_2\ (r_2 + \delta_2 + c_2)[1 - R_p]} \geqslant 1. \tag{3.6}$$

We denote

$$R_p^* = \frac{\alpha_2\ (1-\sigma)\ (\Lambda^* - \Lambda_p)^2}{4\delta_2\mu_2\ (r_2 + \delta_2 + c_2)[1 - R_p]}.$$

Now we look for positive $(\bar{S}_h, \bar{I}_h)$. From 1st and 2nd equation of (3.2) we obtain two forms of $\bar{I}_h$ as

$$\bar{I}_h = \frac{\Lambda_h - \mu_1\bar{S}_h}{\mu_1 + \delta_1} \text{ and } \bar{I}_h = \frac{\alpha_1\ (1-\sigma)\bar{S}_h\bar{I}_p}{(\mu_1 + \delta_1) - \beta_1\ (1-\sigma)\bar{S}_h} \tag{3.7}$$

respectively. Equating the above two we obtain a quadratic equation in $\bar{S}_h$ of the form

$$B_0\ (\bar{S}_h)^2 + B_1\bar{S}_h + B_2 = 0, \tag{3.8}$$

TABLE 3. Condition of existence of endemic equilibrium in system (2.1).

| Case | $R_p$ | $\Lambda_p$ | $R_p^*$ | No. of $\mathcal{D}_1$ | $R_h^*$ | No. of $\mathcal{D}_{11}$ |
|---|---|---|---|---|---|---|
| 1 | $>1$ | $\leqslant \Lambda^*$ | $>1$ | 1 | $=1$<br>$>1$ | 1<br>2 |
| 2 | $>1$ | $>\Lambda^*$ | $>1$ | 1 | $=1$<br>$>1$ | 1<br>2 |
| 3 | $=1$ | $>\Lambda^*$ | $>1$ | 1 | $=1$<br>$>1$ | 1<br>2 |
| 4 | $<1$ | $>\Lambda^*$ | $>1$ | 2 | $=1$<br>$>1$ | 2<br>4 |
| 5 | $<1$ | $>\Lambda^*$ | $=1$ | 1 | $=1$<br>$>1$ | 1<br>2 |

where

$$\begin{aligned} B_0 &= \beta_1\ (1-\sigma)\mu_1 \\ B_1 &= -[\alpha_1\ (1-\sigma)\mu_1\bar{I}_p + \mu_1\ (\mu_1+\delta_1) + \Lambda_h\beta_1\ (1-\sigma)] \\ B_2 &= \ (\mu_1+\delta_1)\Lambda_h. \end{aligned}$$

As the equation has no negative root, the discriminant sign will determine the existence of $\mathcal{D}_{11}$. Now,

$$B_1^2 - 4B_0B_2 \lessgtr 0$$

which implies

$$\frac{\alpha_1\ (1-\sigma)\mu_1\bar{I}_p + \mu_1\ (\mu_1+\delta_1) + \Lambda_h\beta_1\ (1-\sigma)}{2\sqrt{\beta_1\ (1-\sigma)\mu_1\ (\mu_1+\delta_1)\Lambda_h}} \lessgtr 1$$

Denote,

$$R_h^* = \frac{\alpha_1\ (1-\sigma)\mu_1\bar{I}_p + \mu_1\ (\mu_1+\delta_1) + \Lambda_h\beta_1\ (1-\sigma)}{2\sqrt{\beta_1\ (1-\sigma)\mu_1\ (\mu_1+\delta_1)\Lambda_h}}$$

**Remark 3.4.** If $R_h^* < 1$, $\mathcal{D}_{11}$ will not exist even if endemic equilibrium of animal subsystem $\mathcal{D}_1 = \ (\bar{S}_p, \bar{I}_p)$ exists. So, $R_h^* \geqslant 1$ is the condition of existence of at least one endemic equilibrium $\mathcal{D}_{11}$.

It is observed that if $\bar{I}_p = 0$ the condition $R_h^* > 1$ for existence of $\ (\bar{S}_h, \bar{I}_h)$ will reduce to $R_h > 1$ (*i.e.*. condition for existence of $\mathcal{D}_{10}$). We assemble the results of the above discussion about $\mathcal{D}_{11}$ in Table 3. If $\mathcal{D}_{11} = \ (\bar{S}_h, \bar{I}_h, \bar{S}_p, \bar{I}_p)$ exists $\bar{S}_h$ and $\bar{I}_p$ will be obtained by solving the quadratic equations (3.8) and (3.4). $\bar{S}_p$ and $\bar{I}_h$ are given by (3.3) and (3.7) respectively.

### 3.3. Local stability of equilibria

In this section the stability property of various equilibria is studied. Let $\ (\bar{S}_h, \bar{I}_h, \bar{S}_p, \bar{I}_p)$ be an equilibrium point. The Jacobian matrix at this point is

$$\begin{pmatrix} J_h & J_k \\ \mathbf{0} & J_p \end{pmatrix} \tag{3.9}$$

where

$$J_h = \begin{pmatrix} -\beta_1\ (1-\sigma)\bar{I}_h - \alpha_1\ (1-\sigma)\bar{I}_p - \mu_1 & -\beta_1\ (1-\sigma)\bar{S}_h \\ \beta_1\ (1-\sigma)\bar{I}_h + \alpha_1\ (1-\sigma)\bar{I}_p & \beta_1\ (1-\sigma)\bar{S}_h - \mu_1 - \delta_1 \end{pmatrix} \tag{3.10}$$

and

$$J_p = \begin{pmatrix} -\alpha_2\ (1-\sigma)\bar{I}_p - \mu_2 & -\alpha_2\ (1-\sigma)\bar{S}_p + r_2 \\ \alpha_2\ (1-\sigma)\bar{I}_p & \alpha_2\ (1-\sigma)\bar{S}_p - r_2 - \delta_2 - \frac{c_2}{(1+\bar{I}_p)^2} \end{pmatrix} \tag{3.11}$$

and

$$J_k = \begin{pmatrix} 0 & -\alpha_1\ (1-\sigma)\bar{S}_h \\ 0 & \alpha_1\ (1-\sigma)\bar{S}_h \end{pmatrix}.$$

It is to be noted that the characteristic equation of (3.9) will take the structure $|J_h - \lambda I_2||J_p - \lambda I_2| = 0$.

**Theorem 3.5.** *The disease free equilibrium $\mathcal{D}_{00}$ is Locally Asymptotically Stable (LAS) if $R_0 < 1$ and unstable if $R_0 > 1$.*

*Proof.* Recall $R_0 = \max\{R_h, R_p\}$, where $R_h = \frac{\Lambda_h \beta_1\ (1-\sigma)}{\mu_1\ (\mu_1+\delta_1)}$ and $R_p = \frac{\Lambda_p \alpha_2\ (1-\sigma)}{\mu_2\ (r_2+\delta_2+c_2)}$. At $\mathcal{D}_{00}$, $\bar{S}_h = \frac{\Lambda_h}{\mu_1}$, $\bar{I}_h = 0$, $\bar{S}_p = \frac{\Lambda_p}{\mu_2}$, $\bar{I}_p = 0$. Substituting in (3.10) and (3.11) we calculate the eigen values by equating each determinant to 0. The eigen values are $-\mu_1,\ (\mu_1+\delta_1)\ (R_h - 1), -\mu_2,\ (r_2+\delta_2+c_2)\ (R_p - 1)$. For negativity of all eigen values, $R_0 < 1$, which ensures LAS $\mathcal{D}_{00}$. If $R_0 > 1$ at least one eigen value is positive, confirming instability of $\mathcal{D}_{00}$. □

**Theorem 3.6.** *The boundary equilibrium $\mathcal{D}_{10}$ is LAS if $R_p < 1$ and unstable if $R_p > 1$.*

*Proof.* $\mathcal{D}_{10}$ exists if $R_h > 1$ and $R_p \neq 1$. Here $\bar{S}_h = \frac{\mu_1+\delta_1}{\beta_1\ (1-\sigma)}$, $\bar{I}_h = \frac{(R_h-1)\mu_1}{\beta_1\ (1-\sigma)}$, $\bar{S}_p = \frac{\Lambda_p}{\mu_2}$, $\bar{I}_p = 0$. After substituting in (3.10), we observe that the tr $(J_h) < 0$ and det $(J_h) > 0$ *i.e.*. the eigen values have negative real part. The eigen values for $J_p$ are $-\mu_2,\ (r_2+\delta_2+c_2)\ (R_p - 1)$ which implies LAS $\mathcal{D}_{10}$ will exist if $R_p < 1$ and unstable $\mathcal{D}_{10}$ will exist if $R_p > 1$. □

Now we state and prove a sufficient condition of LAS of $\mathcal{D}_{11}$.

**Theorem 3.7.** *The endemic equilibrium $\mathcal{D}_{11}$ is LAS if*

$$\bar{I}_p \geqslant \frac{c_2 - \mu_2}{\alpha_2\ (1-\sigma)} \text{ and } (1+\bar{I}_p)^2 > \frac{\mu_2 c_2 - c_2\alpha_2\ (1-\sigma)}{\delta_2\alpha_2\ (1-\sigma)}.$$

*Proof.* We first study the stability of $\mathcal{D}_1$ in animal subsystem. Assuming $\mathcal{D}_1 = (\bar{S}_p, \bar{I}_p)$ exists,

$$\begin{aligned} \text{the trace tr } (J_p) &= -\alpha_2\ (1-\sigma)\bar{I}_p - \mu_2 + \alpha_2\ (1-\sigma)\bar{S}_p - r_2 - \delta_2 - \frac{c_2}{(1+\bar{I}_p)^2} \\ &< -\alpha_2\ (1-\sigma)\bar{I}_p - \mu_2 + c_2. \\ \text{So, tr } (J_p) < 0 \text{ if } \bar{I}_p &\geqslant \frac{c_2 - \mu_2}{\alpha_2\ (1-\sigma)}. \end{aligned} \tag{3.12}$$

$$\text{The determinant det } (J_p) = \bar{I}_p\left[\delta_2\alpha_2\ (1-\sigma) - \frac{\mu_2 c_2 - c_2\alpha_2\ (1-\sigma)}{(1+\bar{I}_p)^2}\right].$$

$$\text{Evidently, det } (J_p) > 0 \text{ if } (1+\bar{I}_p)^2 > \frac{\mu_2 c_2 - c_2\alpha_2\ (1-\sigma)}{\delta_2\alpha_2\ (1-\sigma)}. \tag{3.13}$$

If (3.12) and (3.13) are satisfied, the eigen values for animal subsystem have negative real part *i.e.*. $\mathcal{D}_1$ of animal subsystem is LAS. We observe after simplification of the trace and determinant of $J_h$ that, tr $(J_h) < 0$ and det $(J_h) > 0$ unconditionally. So locally stable $\mathcal{D}_1$ ensures local stability of $\mathcal{D}_{11}$ whenever it exists. □

### 3.4. Global stability of animal subsystem

**Theorem 3.8.** *The disease free equilibrium of the animal subsystem* $\mathcal{D}_0 = \left(\frac{\Lambda_p}{\mu_2}, 0\right)$ *is globally asymptotically stable if* $R_p < 1$ *and any one of the following two conditions hold*

*(i)* $\Lambda_p \leqslant \Lambda^*$ ,
*(ii)* $\Lambda_p > \Lambda^*$ *and* $R_p^* < 1$.

*Proof.* From lemma 3.1 we assert that the region $\Theta = \left\{ (S_p, I_p) \in \mathbb{R}^2_+ : 0 < S_p + I_p \leqslant \frac{\Lambda_p}{\mu_2} \right\}$ is positively invariant attractor set. From Table 2 it is evident that if either condition *(i)* or *(ii)* is satisfied along with $R_p < 1$, then the animal subsystem has no endemic equilibrium *i.e.*. $(\frac{\Lambda_p}{\mu_2}, 0)$ is the only equilibrium point. Furthermore this equilibrium point is $LAS$. We deduce from Poincaré-Bendixon theorem that no periodic orbit exist in $\Theta$. So the local stability of $(\frac{\Lambda_p}{\mu_2}, 0)$ implies that the $\omega$-limit set of every solution originating in $\mathbb{R}^2_+$ is the singleton set $\{\mathcal{D}_0\}$. Therefore, the locally stable equilibrium point $(\frac{\Lambda_p}{\mu_2}, 0)$ of animal subsystem is also globally asymptotically stable under the stated conditions. □

## 4. Bifurcation analysis

From the results of above section it is asserted that the stability of $\mathcal{D}_{11}$ is solely dependent on the stability of animal subsystem endemic equilibrium $\mathcal{D}_1$. So we focus on some interesting dynamics originating from animal subsystem. Significantly, it is proved that $\mathcal{D}_1 = (\bar{S}_p, \bar{I}_p)$ can coexist with disease free equilibrium of subsystem$= (\breve{S}_p, 0)$ (Table 2) even if the basic reproduction number $R_p < 1$. Conditions (3.12) and (3.13) imply that stability of $\mathcal{D}_1$ is ensured by number of infected crossing a threshold value. All those facts points towards backward bifurcation.

**Theorem 4.1.** *The Nipah animal-human infection model (2.1) undergoes backward bifurcation at* $R_p = 1$, *if* $R_h < 1$ *and*

$$\frac{1}{\mu_2^2}\left(\mu_2 r_2 - \Lambda_p \alpha_2 \ (1-\sigma) - c_2 \mu_2^2\right) > 0. \tag{4.1}$$

*Proof.* We rewrite the system (2.1) by replacing $S_h, I_h, S_p, I_p$ with $v_1, v_2, v_3, v_4$ respectively, so that we get

$$\begin{aligned}
\dot{v_1} &= \Lambda_h - \beta_1 \ (1-\sigma) v_1 v_2 - \alpha_1 \ (1-\sigma) v_1 v_4 - \mu_1 v_1 &&= g_1 \ (v_1, v_2, v_3, v_4) \\
\dot{v_2} &= \beta_1 \ (1-\sigma) v_1 v_2 + \alpha_1 \ (1-\sigma) v_1 v_4 - \mu_1 v_2 - \delta_1 v_2 &&= g_2 \ (v_1, v_2, v_3, v_4) \\
\dot{v_3} &= \Lambda_p - \alpha_2 \ (1-\sigma) v_3 v_4 - \mu_2 v_3 + r_2 v_4 &&= g_3 \ (v_1, v_2, v_3, v_4) \\
\dot{v_4} &= \alpha_2 \ (1-\sigma) v_3 v_4 - r_2 v_4 - \delta_2 v_4 - c_2 \frac{v_4}{1+v_4} &&= g_4 \ (v_1, v_2, v_3, v_4).
\end{aligned} \tag{4.2}$$

The Jacobian at $\mathcal{D}_{00} = \left(\frac{\Lambda_h}{\mu_1}, 0, \frac{\Lambda_p}{\mu_2}, 0\right)$ is obtained from (3.9). As $R_h < 1$ three of the eigen values are negative. We choose $c_2 = c_2^\star$ such that the 4th eigenvalue $\alpha_2 \ (1-\sigma)\frac{\Lambda_p}{\mu_2} - r_2 - \delta_2 - c_2$ becomes 0. The right eigen vector

$\bar{ev}_{rt} = (ev_{rt1}, ev_{rt2}, ev_{rt3}, ev_{rt4})^T$ for eigen value 0 is given by

$$\begin{cases} ev_{rt1} = \dfrac{(\mu_1+\delta_1)\alpha_1\ (1-\sigma)\Lambda_h}{[\mu_1\ (\mu_1+\delta_1) - \beta_1\ (1-\sigma)\Lambda_h]\mu_1} \\ ev_{rt2} = \dfrac{\alpha_1\ (1-\sigma)\Lambda_h}{\beta_1\ (1-\sigma)\Lambda_h - \mu_1\ (\mu_1+\delta_1)} \\ ev_{rt3} = \dfrac{\alpha_2\ (1-\sigma)\Lambda_p - r_2\mu_2}{\mu_2^2} \\ ev_{rt4} = -1. \end{cases} \tag{4.3}$$

Similarly, the left eigen vector is calculated as $\bar{ev}_{lt} = (ev_{lt1}, ev_{lt2}, ev_{lt3}, ev_{lt4}) = (0,0,0,1)$. The coefficients $a$ and $b$ defined in Theorem 4.1 of [5] are simplified as

$$a = \sum_{i,j=1}^{4} ev_{rti} ev_{rtj} \frac{\partial g_4}{\partial v_i \partial v_j}\ (\mathcal{D}_{00}, c_2^*) = \frac{2}{\mu_2^2}\big(\mu_2 r_2 - \Lambda_p \alpha_2\ (1-\sigma) - c_2\mu_2^2\big) \tag{4.4}$$

and

$$b = \sum_{i=1}^{4} ev_{rti} \frac{\partial g_4}{\partial v_i \partial c_2}\ (\mathcal{D}_{00}, c_2^*) = 1 \tag{4.5}$$

respectively. As $b > 0$ always, sign of $a$ is decisive in the local dynamics around $\mathcal{D}_{00}$. So, by [5], if $a > 0$, backward bifurcation occurs at $R_p = 1$. For $a > 0$ we obtain condition (4.1). □

We further investigate the possibility of Hopf bifurcation,

**Theorem 4.2.** *The endemic equilibrium* $\mathcal{D}_{11} = (\bar{S}_h, \bar{I}_h, \bar{S}_p, \bar{I}_p)$ *undergoes Hopf bifurcation at* $c_2 = c_2^*$ *if and only if*

*(i)* $\frac{c_2^* \bar{I}_p\ (c_2^*)}{(1+\bar{I}_p\ (c_2^*))^2} - \alpha_2\ (1-\sigma)\bar{I}_p\ (c_2^*) - \mu_2 = 0$

*(ii)* $\bar{I}_p\ (c_2^*)\left[\delta_2\alpha_2\ (1-\sigma) - c_2^* \frac{\mu_2 - \alpha_2\ (1-\sigma)}{(1+\bar{I}_p\ (c_2^*))^2}\right] > 0$

*(iii)* $\frac{c_2^*\ (1-\bar{I}_p\ (c_2^*))\bar{I}_p{}'\ (c_2^*)}{(\bar{I}_p\ (c_2^*)+1)^3} + \frac{\bar{I}_p\ (c_2^*)}{(\bar{I}_p\ (c_2^*)+1)^2} - \alpha_2\ (1-\sigma)\bar{I}_p{}'\ (c_2^*) \neq 0.$

*Proof.* The characteristic equation of Jacobian (3.9) takes the form $|J_h - \lambda I_2||J_p - \lambda I_2| = 0$ where $J_h$ and $J_p$ defined by (3.10) and (3.11) respectively. From Theorem 3.7, we infer that the eigen values of $J_h$ will always have negative real part. So, $J_p$ will determine the condition for the presence of purely imaginary eigen values necessary for Hopf bifurcation. Let the bifurcation parameter be $c_2$. The characteristic equation for $J_p$ takes the form $\lambda^2 - \text{tr}\ (J_p)\lambda + \det\ (J_p) = 0$, where

$$\text{tr}\ (J_p) = -\alpha_2\ (1-\sigma)\bar{I}_p - \mu_2 + \frac{c_2\bar{I}_p}{(1+\bar{I}_p)^2} \text{ and } \det\ (J_p) = \bar{I}_p\left[\delta_2\alpha_2\ (1-\sigma) - c_2\frac{\mu_2 - \alpha_2\ (1-\sigma)}{(1+\bar{I}_p)^2}\right].$$

Clearly, $\text{tr}\ (J_p) = 0$ will give purely imaginary eigen value if $\det\ (J_p) > 0$. We find threshold parameter value $c_2^*$ for bifurcation by solving $\text{tr}\ (J_p) = 0$ for $c_2$, which gives us condition (i). The condition (ii) is deduced from

det $(J_p) > 0$. Next the transversality condition of Hopf bifurcation needs to be verified, which is

$$\left.\frac{d\,\mathrm{tr}\,(J_p\,(c_2))}{dc_2}\right|_{c_2=c_2^*} \neq 0.$$

After computation the above expression is transformed to

$$\frac{c_2^*\,(1-\bar{I}_p\,(c_2^*))\bar{I}_p{}'\,(c_2^*)}{(\bar{I}_p\,(c_2^*)+1)^3}+\frac{\bar{I}_p\,(c_2^*)}{(\bar{I}_p\,(c_2^*)+1)^2}-\alpha_2\,(1-\sigma)\bar{I}_p{}'\,(c_2^*)\neq 0$$

which gives the condition (iii). Hence the proof is complete. □

## 5. Optimal control of some adjustable parameters

The economic and social impact of Nipah outbreak has been devastating in the South-east Asian region. Apart from the high mortality in human cases, the culling of pigs almost wiped out the pork industry in this region. As the disease spilled over from animal to human in the farms and abattoirs, the proper management within farm during minor outbreaks is extremely important. For a farm owner implementation of biosecurity measures as well as isolation and treatment of infected pig is heavily influenced by economic factors. In order to identify economically viable time bound infection control strategies, in this section we use Pontryagin's Maximum Principle [34] on the given system. The controllable parameters to be optimized are farmers control ($\sigma$), market supply rate ($\mu_2$) and culling rate ($c_2$). The objective functional of optimal control problem within the time range $[0, t^\star]$ considered here is

$$\min\ \mathcal{J}\,(\sigma,\mu_2,c_2)=\int_0^{t^\star}(w_1I_h+w_2I_p+w_3\sigma^2+w_4\mu_2^2+w_5c_2^2-w_6\mu_2S_p)\mathrm{d}t \tag{5.1}$$

subject to system (2.1) with given initial conditions. It is assumed that the control set

$$\mathcal{U}=\{\,(\sigma,\mu_2,c_2)\in\mathbb{R}_+^3|0\leqslant\sigma\leqslant\sigma_{\max}<1,0<\mu_{2\,\min}\leqslant\mu_2\leqslant 1,0\leqslant c_2\leqslant c_{2\,\max}\}$$

is Lebesgue measurable for $t\in[0,t^\star]$. Cost $w_1$ is considered much higher than $w_2$, as a suspected NiV infection among farm workers causes panic and decline in demand of farm produce for a long time. $w_3$ is the cost of maintenance of biosecurity. We consider $\sigma_{\max}<1$ to rule out ideal case of perfect maintenance. As $\mu_2$ $(>0)$ determines the time of departure of full grown pigs to market, the farmer can control it to curb infection in farm to a certain extent, conceding diminished profit. Culling is the extreme but sometimes necessary measure to counteract disease, which will have huge impact on income of farm. An optimal culling strategy can help retain control over disease with minimum loss. $w_4, w_5$ are the weights attached to $\mu_2$ and $c_2$ respectively. $w_6$ is effective profit from a healthy pig which is supplied to market at rate $\mu_2$. Pointwise minimization of the Hamiltonian

$$\begin{aligned}
&\mathcal{H}\,(t,S_h,I_h,S_p,I_p,k_1,k_2,k_3,k_4,\sigma,\mu_2,c_2)\\
&\quad=w_1I_h+w_2I_p+w_3\sigma^2+w_4\mu_2^2+w_5c_2^2-w_6\mu_2S_p\\
&\quad+k_1\Big[\Lambda_h-\beta_1\,(1-\sigma)S_hI_h-\alpha_1\,(1-\sigma)S_hI_p-\mu_1S_h\Big]\\
&\quad+k_2\Big[\beta_1\,(1-\sigma)S_hI_h+\alpha_1\,(1-\sigma)S_hI_p-\mu_1I_h\,(t)-\delta_1I_h\Big]\\
&\quad+k_3\Big[\Lambda_p-\alpha_2\,(1-\sigma)S_pI_p-\mu_2S_p+r_2I_p\Big]\\
&\quad+k_4\Big[\alpha_2\,(1-\sigma)S_pI_p-r_2I_p-\delta_2I_p-c_2\frac{I_p}{1+I_p}\Big]
\end{aligned}\tag{5.2}$$

with respect to the controls $\sigma, \mu_2, c_2$ leads to the minimization of proposed objective function (5.1). The necessary optimality condition derived applying Pontryagin's Maximum Principle is stated in following theorem.

**Theorem 5.1.** *If control function* $(\hat{\sigma}, \hat{\mu_2}, \hat{c_2})$ *and state variable function* $(\hat{S_h}, \hat{I_h}, \hat{S_p}, \hat{I_p})$ *minimize* $\mathcal{J}$*, then there exist absolutely continuous multipliers* $(k_1, k_2, k_3, k_4) \in \mathbb{R}^4$ *for* $t \in [0, t^\star]$ *such that*

$$\begin{cases} \dfrac{\mathrm{d}k_1}{\mathrm{d}t} = \mu_1 k_1 + \ (k_1 - k_2)\beta_1 \ (1-\sigma) I_h + \ (k_1 - k_2)\alpha_1 \ (1-\sigma) I_p, \\ \dfrac{\mathrm{d}k_2}{\mathrm{d}t} = -w_1 + \ (k_1 - k_2)\beta_1 \ (1-\sigma) S_h + k_2 \ (\mu_1 + \delta_1), \\ \dfrac{\mathrm{d}k_3}{\mathrm{d}t} = \ (k_3 - k_4)\alpha_2 \ (1-\sigma) I_p + k_3\mu_2 + w_6\mu_2, \\ \dfrac{\mathrm{d}k_4}{\mathrm{d}t} = -w_2 + \ (k_1 - k_2)\alpha_1 \ (1-\sigma) S_h + \ (k_3 - k_4)\alpha_2 \ (1-\sigma) S_p + \ (k_4 - k_3) r_2 + k_4\delta_2 + \dfrac{k_4 c_2}{(I_p+1)^2} \end{cases} \tag{5.3}$$

*for almost every* $t \in [0, t^\star]$*, with transversality conditions at final time being* $k_i \ (t^\star) = 0$ *for* $i = 1, 2, 3, 4$*. Furthermore, the optimal values of the controls are expressed as*

$$\hat{\sigma} = \min\left\{ \max\left\{0, \frac{(k_4 - k_3)\alpha_2 \hat{S_p} \hat{I_p} + \ (k_2 - k_1) \ (\alpha_1 \hat{S_h} \hat{I_p} + \beta_1 \hat{S_h} \hat{I_h})}{2w_3} \right\}, \sigma_{\max} \right\} \tag{5.4}$$

$$\hat{\mu_2} = \min\left\{ \max\left\{\mu_{2\min}, \frac{(k_3 + w_6)\hat{S_p}}{2w_4} \right\}, 1 \right\} \tag{5.5}$$

$$\hat{c_2} = \min\left\{ \max\left\{0, \frac{k_4 \hat{I_p}}{2w_5 \ (1 + \hat{I_p})} \right\}, c_{2\max} \right\}. \tag{5.6}$$

*Proof.* By Pontryagin's Maximum Principle, necessary condition for the adjoint system (5.3) of multipliers is obtained from the following equations

$$\frac{\mathrm{d}k_1}{\mathrm{d}t} = -\frac{\partial \mathcal{H}}{\partial S_h}, \frac{\mathrm{d}k_2}{\mathrm{d}t} = -\frac{\partial \mathcal{H}}{\partial I_h}, \frac{\mathrm{d}k_3}{\mathrm{d}t} = -\frac{\partial \mathcal{H}}{\partial S_p}, \frac{\mathrm{d}k_4}{\mathrm{d}t} = -\frac{\partial \mathcal{H}}{\partial I_p} \tag{5.7}$$

along with the transversality condition at final time of the optimizing process. The characterization of the optimal controls $(\hat{\sigma}, \hat{\mu_2}, \hat{c_2})$ on the set $\{0 \leqslant \sigma \leqslant \sigma_{\max} < 1, 0 < \mu_{2\min} \leqslant \mu_2 \leqslant 1, 0 \leqslant c_2 \leqslant c_{2\max}\}$ for $t \in [0, t^\star]$ are based on

$$\frac{\partial \mathcal{H}}{\partial \sigma} = 0, \ \frac{\partial \mathcal{H}}{\partial \mu_2} = 0 \text{ and } \frac{\partial \mathcal{H}}{\partial c_2} = 0 \tag{5.8}$$

respectively. This set of equations generates the following three explicit forms of three optimal controls,

$$\begin{aligned} \sigma^\natural &= \frac{1}{2w_3}[ \ (k_4 - k_3)\alpha_2 \hat{S_p} \hat{I_p} + \ (k_2 - k_1) \ (\alpha_1 \hat{S_h} \hat{I_p} + \beta_1 \hat{S_h} \hat{I_h}) \\ \mu_2^\natural &= \frac{(k_3 + w_6)\hat{S_p}}{2w_4} \\ c_2^\natural &= \frac{k_4 \hat{I_p}}{2w_5 \ (1 + \hat{I_p})}. \end{aligned}$$

By standard arguments involving bounds of control we conclude

$$\hat{\sigma} = \begin{cases} 0, \text{ if } \sigma^{\natural} \leqslant 0 \\ \sigma^{\natural}, \text{ if } 0 < \sigma^{\natural} < \sigma_{\max} \\ \sigma_{\max}, \text{ if } \sigma^{\natural} \geqslant \sigma_{\max} \end{cases}, \ \hat{\mu_2} = \begin{cases} \mu_{2\min}, \text{ if } \mu_2^{\natural} \leqslant \mu_{2\min} \\ \mu_2^{\natural}, \text{ if } \mu_{2\min} < \mu_2^{\natural} < 1 \\ 1, \text{ if } \mu_2^{\natural} \geqslant 1 \end{cases}, \ \hat{c_2} = \begin{cases} 0, \text{ if } c_2^{\natural} \leqslant 0 \\ c_2^{\natural}, \text{ if } 0 < c_2^{\natural} < c_{2\max} \\ c_{2\max}, \text{ if } c_2^{\natural} \geqslant c_{2\max} \end{cases}.$$

This leads to the compact expression of optimal controls in (5.4), (5.5) and (5.6) respectively. □

**Theorem 5.2.** *There exists an unique optimal control set* $(\hat{\sigma}, \hat{\mu_2}, \hat{c_2})$ *along with a solution set* $(\hat{S_h}, \hat{I_h}, \hat{S_p}, \hat{I_p})$ *of the corresponding state system (2.1) that minimizes* $\mathcal{J}(\sigma, \mu_2, c_2)$ *over* $\mathcal{U}$.

The existence of optimal solution is ensured by verifying the conditions stated in the Theorem 4.1 and corollary ([15], chap. III). The uniqueness is validated by the Lipschitz structure and boundedness of the state system (2.1) and the adjoint system (5.3) for small $t^{\star}$.

## 6. Numerical simulation and results

In this section we demonstrate various important numerical results from computer simulation of our model system using Matlab and Mathematica. The time unit for all simulation is considered as weeks. Our system is representative of a medium sized swine farm of capacity $500 - 700$ and farm-worker strength $30 - 60$. The parameter values of $\Lambda_h, \Lambda_p, \mu_1$ are chosen to match farm capacity in infection free state. We choose $\alpha_1, \beta_1$ smaller than $\alpha_2$ for optimal control and sensitivity analysis. The average incubation period of Nipah in human is $1 - 2$ weeks after which the symptoms will be visible. Based on this information we assign as the hospitalization rate $\delta_1$. The range of parameter values and the sources are shown in Table 1.

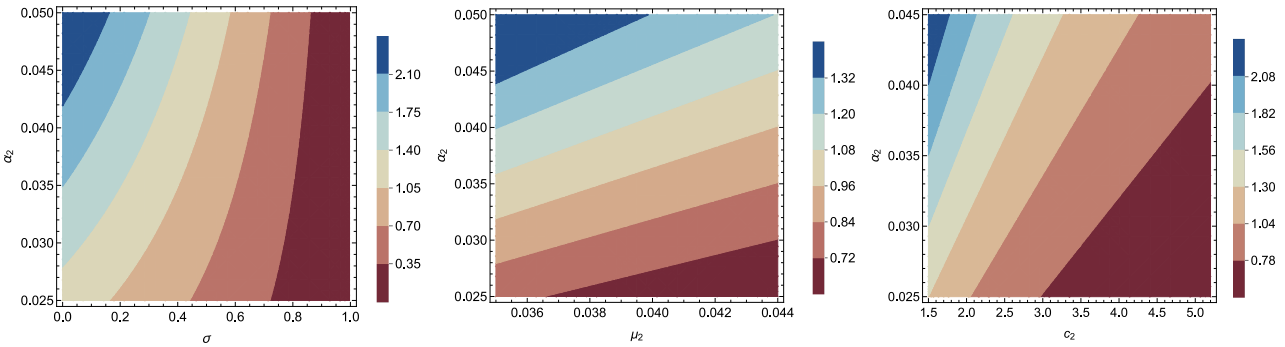


(A) Infection rate from pig to pig ($\alpha_2$) and farmers control ($\sigma$) varied.

(B) Infection rate from pig to pig ($\alpha_2$) and market supply rate ($\mu_2$) varied.

(C) Infection rate from pig to pig ($\alpha_2$) and culling rate ($c_2$) varied.

Figure 2. The contour plot of $R_0$, when pair of parameters are varied. The remaining parameter values are $\Lambda_h = 6, \alpha_1 = 0.023, \beta_1 = 0.021, \mu_1 = 0.16, \delta_1 = 0.5, \Lambda_p = 12, \sigma = 0.5, \alpha_2 = 0.043, r_2 = 0.65, \delta_2 = 0.05, c_2 = 5, \mu_2 = 0.042$.

### 6.1. Variability in $R_0$ with respect to different parameters

In Figure 2 we observe the effect of pair of contrasting parameters in the value of $R_0$, using contour plots. In the figures pig to pig NiV infection rate $\alpha_2$ is compared with the disease inhibitory parameters farmers control ($\sigma$), pig market supply rate ($\mu_2$) and culling rate ($c_2$) respectively. From Figure 2A we observe very high impact of $\sigma$ in bringing down value of $R_0$ below 1, irrespective of value of $\alpha_2$. $c_2$ shows similar but slow effect in this regard (Fig. 2C). From Figure 2B it can be inferred that effect of $\alpha_2$ is dominant over $\mu_2$.

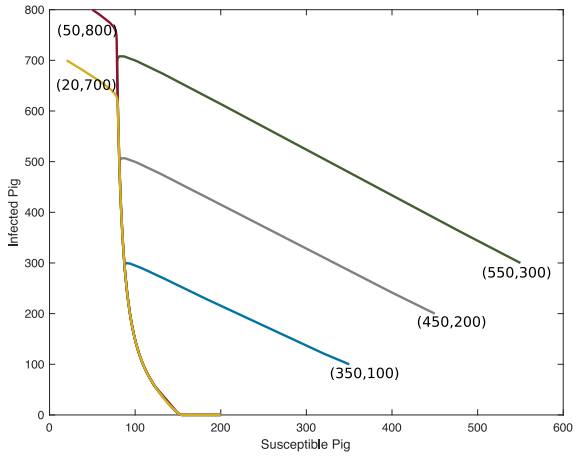


(A) Phase portrait showing global stability of disease-free equilibrium in animal subsystem.

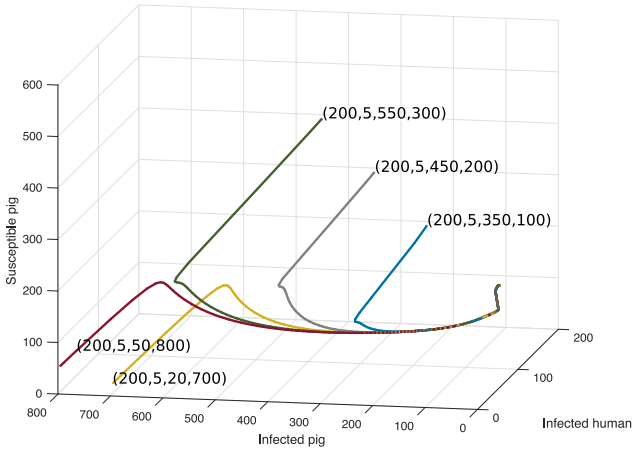


(B) 3D phase-portrait of complete system when animal subsystem disease-free equilibrium is globally stable.

FIGURE 3. The parameter values used for animal subsystem $\Lambda_p = 60, \sigma = 0.3, \alpha_2 = 0.01, r_2 = 0.5, \delta_2 = 0.05, c_2 = 25, \mu_2 = 0.3$. Additional parameter values for full system $\Lambda_h = 10, \alpha_1 = 0.005, \beta_1 = 0.005, \mu_1 = 0.05, \delta_1 = 0.1$.

## 6.2. Global stability of subsystem

In Figure 3A we show that when the conditions stated in Theorem 3.8 are satisfied the disease free equilibrium of animal subsystem $\mathcal{D}_0 = \left(\frac{\Lambda_p}{\mu_2}, 0\right)$ is globally stable. Further in Figure 3B it is demonstrated that global stability of $\mathcal{D}_0$ does not ensure the global stability of disease free equilibrium $\mathcal{D}_{00} = \left(\frac{\Lambda_h}{\mu_1}, 0, \frac{\Lambda_p}{\mu_2}, 0\right)$ in complete system.

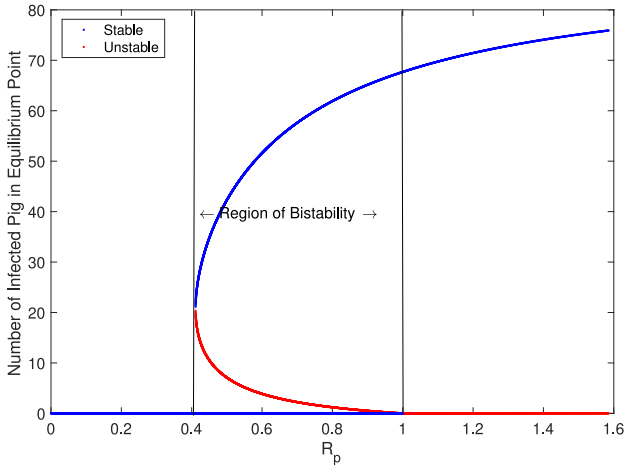


FIGURE 4. Backward Bifurcation of system (2.1) at $R_p = 1$ for parameter values $\Lambda_p = 15, \sigma = 0.40, r_2 = 0.6, \mu_2 = 0.5, \delta_2 = 0.05, \alpha_2 = 0.409$. We choose the remaining parameters such that $R_h < 1$ and $\alpha_1 = 0$.

## 6.3. Bifurcation diagram

In Figure 4 we observe the phenomenon of backward bifurcation, where locally stable disease free equilibrium $\mathcal{D}_{00}$ and boundary equilibrium $\mathcal{D}_{01}$ cohabits even if $R_0 < 1$. The Hopf bifurcation (Fig. 5) is observed for a

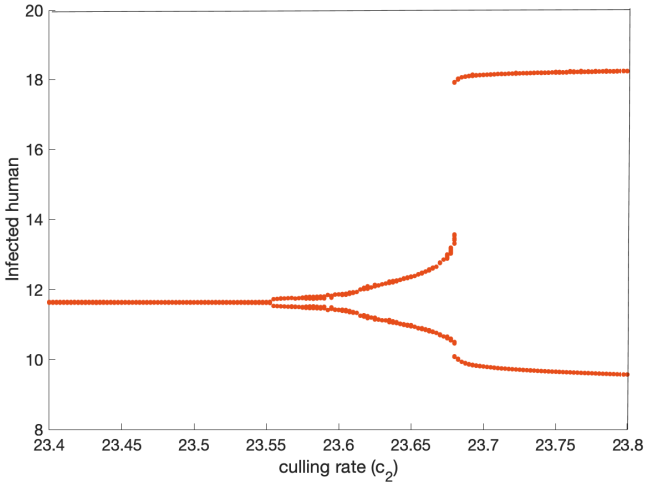


FIGURE 5. Hopf bifurcation of system (2.1) for bifurcation parameter $c_2$ (culling rate) where the other parameter values are $\Lambda_h = 6, \Lambda_p = 21, \sigma = 0.40, \alpha_1 = 0.075, \beta_1 = 0.085; \mu_1 = 0.01, \delta_1 = 0.5, r_2 = 0.7, \delta_2 = 0.05, \alpha_2 = 0.75, \mu_2 = 0.042$.

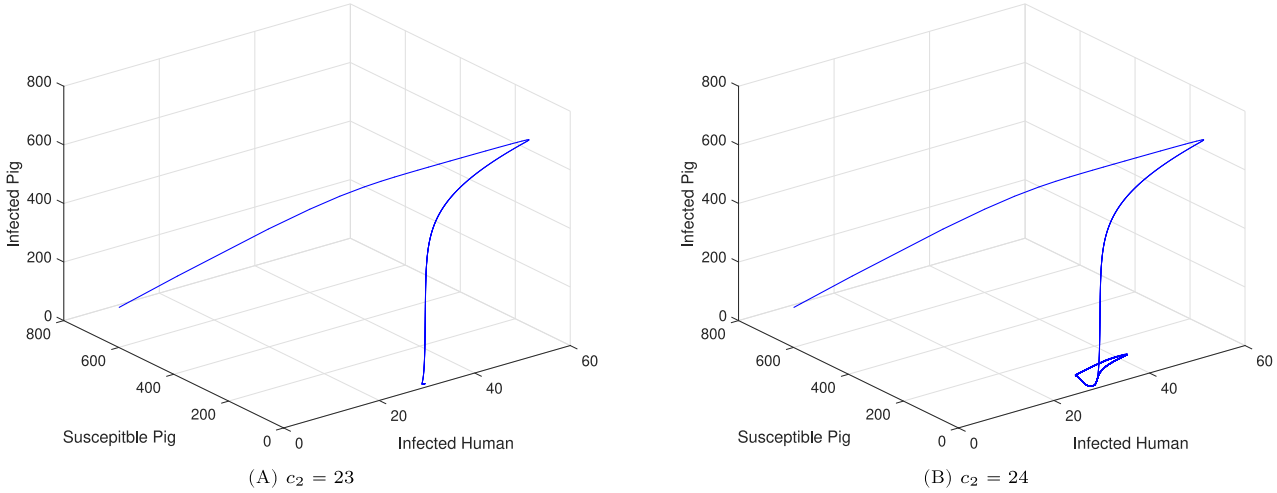


(A) $c_2 = 23$ (B) $c_2 = 24$

FIGURE 6. 3D phase-portrait of system before and after undergoing Hopf bifurcation (Fig. 5) at bifurcation parameter value $c_2 = 23.597338$.

high infection rate and very high culling rate. Using Matcont we obtained the first Lyapunov coefficient value as $-0.01286619$ and the type of Hopf bifurcation is supercritical [18]. The phase portraits (Fig. 6A and B) visualize the occurrence of periodicity and disease persistence at a very low level.

### 6.4. Sensitivity analysis

Now we try to identify those parameters significant for solutions incorporating a certain level of randomness. For this purpose we use statistical method of LHS and PRCC. PRCC quantifies the level of monotonic relation between chosen parameter and solution when the linear effect all other parameters is negated. The techniques are incorporated in a Matlab program provided in [31] and the outcomes are presented by bar diagrams and time series plots.

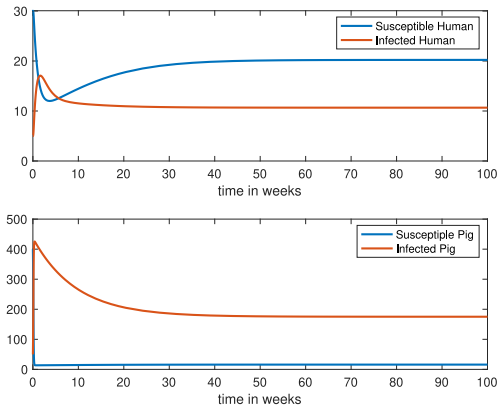


(A) Time series of state variables for the baseline parameter values.

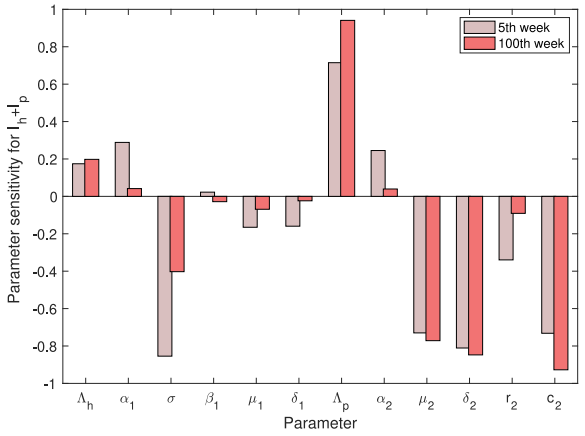


(B) Bar diagram of sensitivity of total infected human and pig measured by PRCC on 5th and last week.

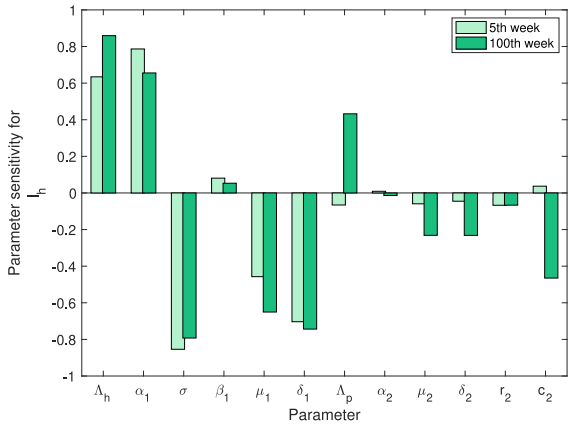


(C) Bar diagram of sensitivity of infected human measured by PRCC on 5th and last week.

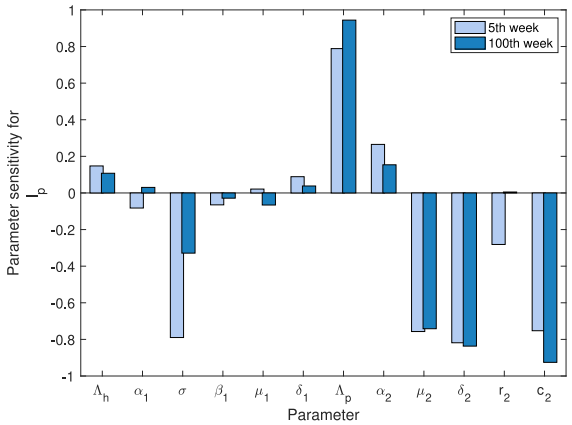


(D) Bar diagram of sensitivity of infected pig measured by PRCC on 5th and last week.

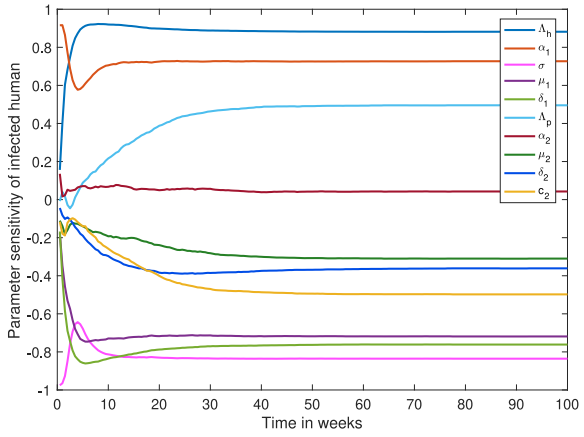


(E) Change of PRCC values of significant parameters with time for infected human.

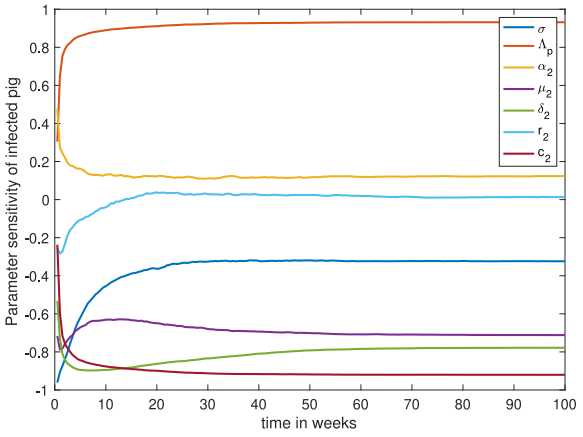


(F) Change of PRCC values of significant parameters with time for infected pig.

FIGURE 7. The plots related to the parameter sensitivity analysis of state variables $I_h$, $I_p$ with baseline parameter values $\Lambda_h = 10, \Lambda_p = 30, \sigma = 0.5, \alpha_1 = 0.007, \beta_1 = 0.005, \mu_1 = 0.16, \delta_1 = 0.5, r_2 = 0.6, \delta_2 = 0.1, \alpha_2 = 0.075, \mu_2 = 0.042, c_2 = 12$. The initial value is $(30, 5, 400, 50)$, the sample size is 200 and level of significance is 0.05.

The baseline values of parameters are given in Figure 7. We select uniform distribution for $\Lambda_h, \Lambda_p$ and all other parameters are assigned normal distribution with moderate variance. From Figure 7A we determine the two time points of interest as 5th week (transient state) and final week (stable state). In Figure 7B the sensitivity plots of total infected pig and human in the system is presented. Pig recruitment parameter $\Lambda_p$ has a very strong and human recruitment parameter $\Lambda_h$ has moderately strong positive relation in both time points. On the contrary $\mu_2, \delta_2, c_2$ has strong negative relation at both time points. At final time farmer's control ($\sigma$) has lost a very strong negative influence of transient state. In Figure 7C and D we observe the parameter correlation with two infected populations separately. Most of the human specific parameters ($\Lambda_h, \alpha_1, \mu_1, \delta_1$) are exhibiting very strong correlation with infected human. As animal subsystem is independent of human influence, strong parametric influences are observed only for $\Lambda_p, \mu_2, \delta_2, c_2$. We find that recovery rate $r_2$ is important in disease eradication of pig subsystem during initial outbreak but become irrelevant once steady state is achieved. The farmers control ($\sigma$) is the only parameter having huge significance in infection control for both human and pig. In Figure 7E and F the PRCC values of statistically significant parameters are plotted for the entire time period to reveal change of sensitivity along with solution trajectory (Fig. 7A). We observed that since the onset of infection $\sigma$ and $\alpha_1$ has maintained almost equal and opposite influence on infected human. Other parameters raised their impact through the entire transient state and then settled. For pig population market sending rate ($\mu_2$) is the only parameter to maintain strong influence as the time progresses. A few parameters ($\alpha_2, r_2, \sigma$) lost their impact during transient state. The effect of $\Lambda_p$ and $c_2$ are almost equal and opposite on infected pig population.

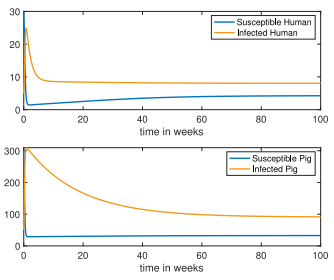


(A) Time series of system variables without optimal control

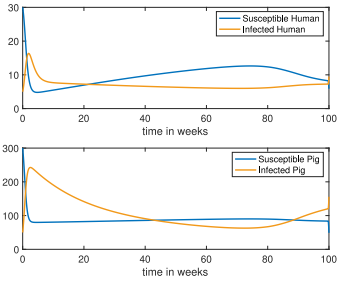


(B) Time series of system variables under optimal control

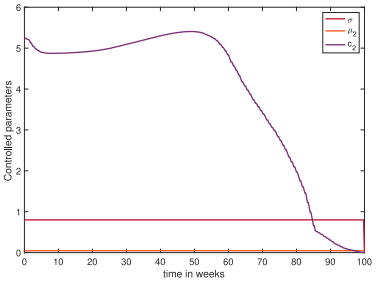


(C) The trajectory of control parameters

FIGURE 8. The system plot with parameter values $\Lambda_h = 6, \Lambda_p = 12, \alpha_1 = 0.023, \beta_1 = 0.021, \mu_1 = 0.16, \delta_1 = 0.5, r_2 = 0.65, \delta_2 = 0.05, \alpha_2 = 0.043$. The initial value is $(30, 5, 300, 50)$ and the weights in objective functional for optimal control are $w_1 = 1, w_2 = 0.2, w_3 = 0.5, w_4 = 0.3, w_5 = 0.45, w_6 = 0.1$. The range of optimally controlled parameters are $0 \leqslant \sigma \leqslant 0.8, 0.035 \leqslant \mu_2 \leqslant 0.046, 0 \leqslant c_2 \leqslant 7$.

## 6.5. Optimal control

In this segment we demonstrate the numerical results from the computer simulation of the optimal control problem in Section 5. To simulate optimal control, forward-backward sweep algorithm [28] is implemented in Matlab program. In Figure 8A and B comparison of the solution trajectory with and without optimal control affirms the positive impact of optimal control in arresting infection. Figure 8C depicts the trajectory of controls in the loss minimization process. It is noted that in optimally controlled system $\sigma$ and $\mu_2$ maintained the highest available value for almost entire control period. But $c_2$ trajectory follows a nonlinear path. We now try to compare the effect of $c_2$ individually or together with one or two optimal controls.

For comparison the three situations considered are as mentioned in Figure 9. From the perspective of infection control it is established in Figure 9A that the market sending parameter is not significant when other two optimal controls are in play. But $c_2$ is only effective in human infection control when $\sigma$ is available at highest level. In Figure 9B we observe similar situation but $\mu_2$ shows better impact in pig infection control in the second half of

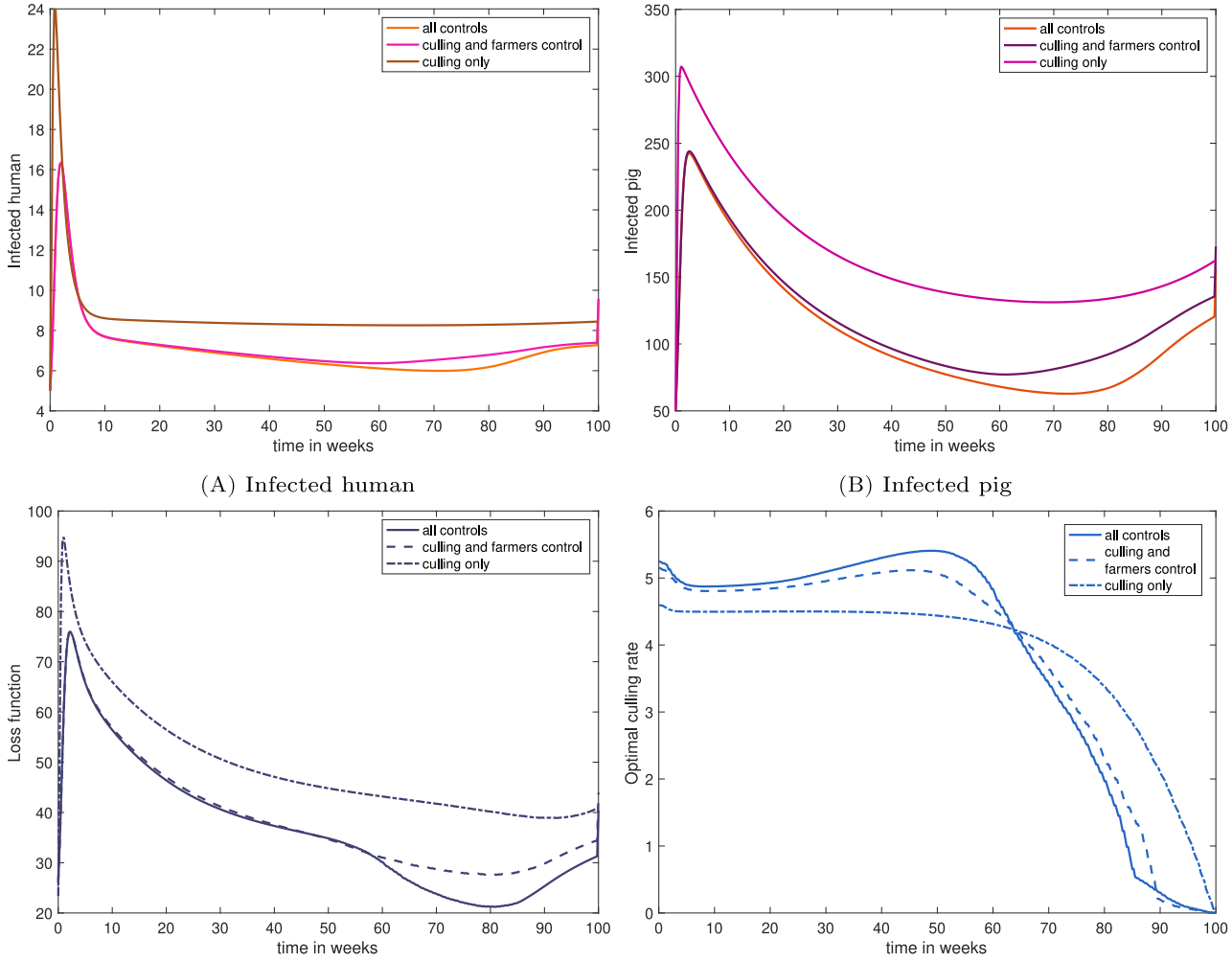


(A) Infected human

(B) Infected pig

(C) Optimal loss function

(D) Optimal culling rate

FIGURE 9. The time series plot of three different control scenarios i) $\sigma, \mu_2, c_2$ optimally controlled, ii) $\sigma, c_2$ optimally controlled and $\mu_2 = 0.042$, iii) $c_2$ optimally controlled and $\mu_2 = 0.042, \sigma = 0.5$. Remaining parameters, weights and initial conditions same as Figure 8.

time span. The economic objective function showed similar trend as infected pig (Fig. 9C). The culling rate ($c_2$) control together with one or more control generates very different trajectory compared to single application. Significantly this control is never applied at the highest available rate and when applied individually as optimal control the maximum applied value was less than that for other two cases (Fig. 9D).

Now we test the sensitivity of the objective function ($\mathcal{J}$ $(\sigma, \mu_2, c_2)$) value [17] towards the uncontrolled parameters in the three cases (Fig. 9), using the LHS and PRCC technique with level of significance 0.01. When all three controls are applied we find that NiV induced death rate ($\delta_2$) is most effective in reduction of loss (Fig. 10A). On the other hand, $\Lambda_h, \Lambda_p$ strongly contribute towards loss. The situation is almost unchanged for two controls (Fig. 10B), where influence of $\alpha_2$ is more. The sensitivity pattern changes for the case of single control. It is observed that when $\sigma$ is not optimally controlled, it has very strong discordant relation with loss function (Fig. 10C). Only one parameter ($\Lambda_p$) has strong relation with increasing loss in this case.

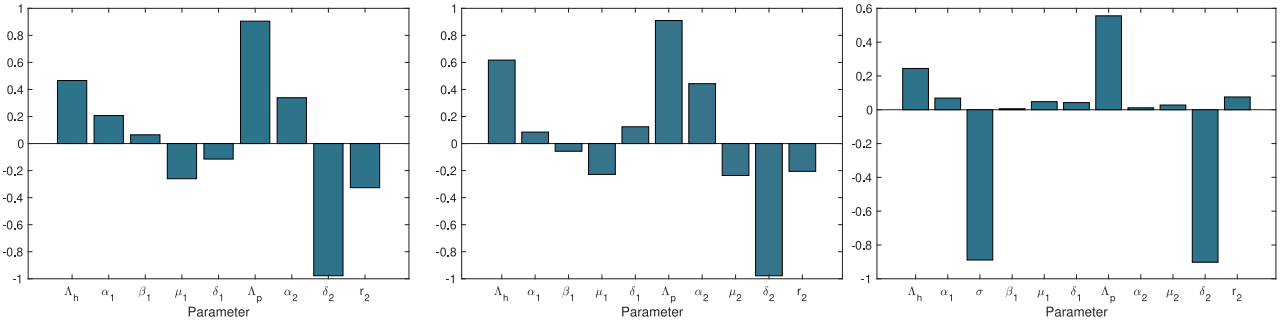


(A) $\sigma, \mu_2, c_2$ optimally controlled (B) $\sigma, c_2$ optimally controlled (C) $c_2$ optimally controlled

FIGURE 10. Bar diagram of PRCC values of optimal objective function with respect to the free parameters in optimal control problem. Baseline parameter values are as mentioned in three cases of Figure 9. The sample size taken is 130 and level of significance is 0.01.

## 7. Discussion

In this paper, we propose a pig-human NiV transmission model inside a commercial farming environment. To the best of our knowledge, such type of NiV model is not studied before, although pig infection and subsequent infection transfer to human magnifies significantly the possibility of epidemic. We have calculated the basic reproduction number $R_0$ which is maximum of two quantities defined in (3.1). Among these two quantities, $R_p$ independently acts as basic reproduction number of animal subsystem. Numerically, we have demonstrated the effect of three pairs of parameters on $R_0$. The infection combatant parameters were again used for optimal control and their level of effectiveness were reiterated.

We have demonstrated the existence of disease free equilibrium, partial endemic boundary equilibrium and unique or multiple endemic equilibriums under different conditions. The existence of endemic equilibrium in animal subsystem may not ensure existence of endemic equilibrium in original system. It is proved that local stability of endemic equilibrium of animal subsystem is enough to ensure local stability of endemic equilibrium of original system. Also it is observed that, when disease free state among pigs is globally stable it may not lead to global stability of disease-free state of humans. Our model exhibits backward bifurcation phenomenon. It implies that the disease is difficult to be eradicated if initial number of infected is high. The Hopf bifurcation occurs when the parameter culling rate ($c_2$) crosses the threshold value. The combination of high infection and higher culling rate has resulted in periodicity of infected population at a very low level. This situation arises when infection rate is high, but the owner not taking prior adequate biosecurity measures, is forced to increase culling excessively. Even this measure fails to eradicate disease completely.

Optimal control theory is used to formulate a viable strategy for farm owner to keep disease under control. The controls are optimized for minimum loss during outbreak. Relative to the chosen weights in objective function, the maintenance of highest biosecurity level even at high economic investment is key to minimization of loss and reduction of infection in human and pig. It is observed that in presence of infection, market sending of uninfected pigs faster than normal time will be beneficial in long run. Culling is more effective together with biosecurity measures and controlled market despatch of pigs on regular basis. Without any other control, culling needs to be applied at a fixed moderate rate for a long period. But this is the least cost-effective strategy to control infection and should be used as the extreme measure for disease control.

The global sensitivity analysis of infected compartment of pig and human population has yielded some important observations. We are able to identify the critical parameter responsible for disease prevalence or decline under uncertainty. Among the two infection rates for human, pig-originated infection rate is observed to be the dominant one. From the time dependent plot of sensitivity we discover that high infection in the beginning coincides with extremely negligible influence of most parameters. This implies that the system trajectory in transient state is primarily influenced by initial condition. The stable state is not achieved until the parameters

gain control over output. In this paper we also performed the sensitivity of total loss value during optimal control process by incorporating LHS and PRCC in optimal control simulation. It is observed that, increment in NiV induced death rate of pigs will reduce total economic loss. This can be explained by direct or indirect impact of total number of infected pigs over various costs associated with infection. A small increment in death rate of pigs lowers infected pig population slightly. But decline in secondary infection of human and pig leads to a high accumulated savings in cost over the total time of control. The equivalent opposite impact of pig recruitment rate can be similarly explained. These facts suggest that the resident pig herd size is crucial in minimizing loss. So the prevalent practice of overcrowding of pigs beyond capacity is detrimental during outbreak. A sensible approach in this direction is to minimize the weekly influx of pigs and to despatch healthy pigs at the earliest opportunity.

The results obtained in this study put extreme importance on farmers overall control in terms of biosecurity measures ($\sigma$), timing of despatch ($\mu_2$) and culling ($c_2$), strengthening the role of informed decision for disease eradication in a farm unit. Such measures may ultimately prevent epidemic in community. These controls directly affect the 'critical herd size', which is crucial in infection persistence as established in a data based study [33], which validates our finding. We can observe the direct impact of biosecurity measures in Malaysia, where since 2001 not a single case of Nipah is reported. Since the outbreak, Malaysian government closed down largely unorganized and traditional pig farms. Farms were relocated to 'identified pig farming areas' where better biosecurity and modern farming practices are encouraged [27]. The authority also took measures to control the number of pigs in farm and banned fruit plantation around the farming areas [12]. This real life evidence is corroborated by our study and acts as a benchmark for farming establishments across the regions susceptible to Nipah infection. There is a scope of enhancement of this work by incorporating parameters like delay in culling, isolation of infected pigs etc.

## References


[1] F.B. Agusto, Mathematical model of Ebola transmission dynamics with relapse and reinfection. *Math. Biosci.* **283** (2017) 48–59.

[2] M.E. Alexander, C. Bowman, S.M. Moghadas, R. Summers, A.B. Gumel and B.M. Sahai, A vaccination model for transmission dynamics of influenza. *SIAM J. Appl. Dyn. Syst.* **3** (2004) 503–524.

[3] M.H.A. Biswas, Optimal control of Nipah virus (NIV) infections: A Bangladesh scenario. *J. Pure Appl. Math.* **12** (2014) 77–104.

[4] M.H.A. Biswas, M.M. Haque and G. Duvvuru, A mathematical model for understanding the spread of Nipah fever epidemic in Bangladesh. In *2015 International Conference on Industrial Engineering and Operations Management (IEOM)* (2015) 1–8.

[5] C. Castillo-Chavez and B. Song, Dynamical models of Tuberculosis and their applications. *Math. Biosci. Eng.* **1** (2004) 361–404.

[6] N.S. Chong and R.J. Smith, Modeling avian influenza using Filippov systems to determine culling of infected birds and quarantine. *Nonlinear Anal.: Real World Appl.* **24** (2015) 196–218.

[7] E.M.C. DÁgata , G.F. Webb and J. Pressley, Rapid emergence of co-colonization with community-acquired and hospital-acquired methicillin-resistant Staphylococcus aureus strains in the hospital setting. *MMNP* **5** (2010) 76–93.

[8] E.M.C. D'Agata, M. Horn and G. Webb, Quantifying the impact of bacterial fitness and repeated antimicrobial exposure on the emergence of multidrug-resistant gram-negative bacilli. *MMNP* **2** (2007) 129–142.

[9] S. Das, P. Das and P. Das, Dynamics and control of multidrug-resistant bacterial infection in hospital with multiple delays. *Commun. Nonlinear Sci. Numer. Simul.* **89** (2020) 105279.

[10] P. Das, P. Das and S. Das, Effects of delayed immune-activation in the dynamics of tumor-immune interactions. *MMNP* **15** (2020) 45.

[11] E. de Wit and V.J. Munster, Animal models of disease shed light on Nipah virus pathogenesis and transmission. *J. Pathol.* **235** (2015) 196–205.

[12] M. Deka and N. Morshed, Mapping disease transmission risk of Nipah virus in south and Southeast Asia. *Trop. Med. Infect. Disease* **3** (2018) 05.

[13] G. Djatcha Yaleu, S. Bowong, E. Houpa Danga and J. Kurths, Mathematical analysis of the dynamical transmission of Neisseria meningitidis serogroup A. *Int. J. Comput. Math.* **94** (2017) 2409–2434.

[14] P.R. Epstein, Climate change and emerging infectious diseases. *Microb. Infection* **3** (2001) 747–754.

[15] W.H. Fleming and R.W. Rishel, Deterministic and stochastic optimal control. Applications of mathematics. Springer-Verlag (1975).

[16] Food and Agriculture Organization of the United Nations. Farmer's Hand Book on Pig Production (2009).

[17] B. Gomero, *Latin hypercube sampling and partial rank correlation coefficient analysis applied to an optimal control problem.* Master's thesis, University of Tennessee, Knoxville (2012).
[18] J. Guckenheimer and P. Holmes, Nonlinear Oscillations, Dynamical Systems, and Bifurcations of Vector Fields. *Applied Mathematical Sciences*. Springer, New York (1983).
[19] A.B. Gumel, Global dynamics of a two-strain Avian influenza model. *Int. J. Comput. Math.* **86** (2009) 85–108.
[20] H. Gulbudak and M. Martcheva, Forward hysteresis and backward bifurcation caused by culling in an Avian influenza model. *Math. Biosci.* **246** (2013) 202–212.
[21] E.V. Grigorieva and E.N. Khailov, Optimal vaccination, treatment, and preventive campaigns in regard to the SIR epidemic model. *MMNP* **9** (2014) 105–121.
[22] E.V. Grigorieva, E.N. Khailov and A. Korobeinikov, Optimal control for a SIR epidemic model with nonlinear incidence rate. *MMNP* **11** (2016) 89–104.
[23] J.M. Hassell, M. Begon, M.J. Ward and E.M. Fèver, Urbanization and disease emergence: Dynamics at the wildlife-livestock-human interface. *Trends Ecol. Evol.* **32** (2017) 55–67.
[24] J.M. Hughes, M.E. Wilson, E.S. Gurley, M. Jahangir Hossain and S.P. Luby, Transmission of Human Infection with Nipah Virus. *Clin. Infect. Dis.* **49** (2009) 1743–1748.
[25] T.T.T. Huynh, A. Aarnink, A. Drucker and M. Verstegen, Pig production in Cambodia, Laos, Philippines, and Vietnam: a review. *Asian J. Agric. Dev.* **4** (2007).
[26] Q. Hu and X. Zou, Optimal vaccination strategies for an influenza epidemic model. *J. Biol. Syst.* **21** (2013) 1340006.
[27] A.B. Jamaluddin and A.B. Adzhar, Nipah virus infection-Malaysia experience, 2011. Accessed on March (2019).
[28] S. Lenhart and J.T. Workman, Optimal Control Applied to Biological Models. CRC Press (2007).
[29] B. Levy, C. Edholm, O. Gaoue, R. Kaondera-Shava, M. Kgosimore, S. Lenhart, B. Lephodisa, E. Lungu, T. Marijani and F. Nyabadza, Modeling the role of public health education in Ebola virus disease outbreaks in Sudan. *Infect. Dis. Model.* **2** (2017) 323–340.
[30] L.-M. Looi and K.-B. Chua, Lessons from the Nipah virus outbreak in Malaysia. *Malaysian J. Pathol.* **29** (2007) 63–67.
[31] S. Marino, I. Hogue, C. Ray and D. Kirschner, A methodology for performing global uncertainty and sensitivity analysis in systems biology. *J. Theor. Biol.* **254** (2008) 178- 196.
[32] M.K. Mondal, M. Hanif and Md. Haider Ali Biswas, A mathematical analysis for controlling the spread of Nipah virus infection. *Int. J. Model. Simul.* **37** (2017) 185–197.
[33] V. Pitzer, R. Aguas, S. Riley, W. Loeffen, J. Wood and B.T. Grenfell, High turnover drives prolonged persistence of influenza in managed pig herds. *J. Royal Soc. Interface* **13** (2016) 20160138.
[34] L.S. Pontryagin, V.G. Boltyanskii, R.V. Gamkrelidze and E.F. Mishchenko, The Mathematical Theory of Optimal Processes. John Wiley & Sons (1962).
[35] B.A. Satterfield, B.E. Dawes and G.N. Milligan, Status of vaccine research and development of vaccines for Nipah virus. *Vaccine* **34** (2016) 2971–2975.
[36] H.J. Shimozako, J. Wu and E. Massad, Mathematical modelling for zoonotic Visceral Leishmaniasis dynamics: a new analysis considering updated parameters and notified human Brazilian data. *Infectious Disease Model* **2** (2017) 143–160.
[37] P. van den Driessche and J. Watmough, Further Notes on the Basic Reproduction Number. Springer Berlin Heidelberg, Berlin, Heidelberg (2008).
[38] L. Wang and G.S. Crameri, Emerging zoonotic viral diseases. *Rev. Sci. Tech.* **33** (2014) 569–581.
[39] H. Weingartl, Hendra and Nipah viruses: pathogenesis, animal models and recent breakthroughs in vaccination. *Vaccine: Dev. Therapy* **59** (2015) 09.
[40] A.K. Wiethoelter, D. Beltrán-Alcrudo, R. Kock and S.M. Mor, Global trends in infectious diseases at the wildlife-livestock interface. *Proc. Natl. Acad. Sci.* **112** (2015) 9662–9667.
[41] A. Wiratsudakul, P. Suparit and C. Modchang, Dynamics of Zika virus outbreaks: an overview of mathematical modeling approaches. *PeerJ* **6** (2018) e4526.